Liquid Crystals
Publication details, including instructions for authors and subscription information:
http://www.informaworld.com/smpp/title~content=t713926090

The influence of sodium chloride on the self-association and chromonic mesophase formation of Edicol Sunset Yellow

J. W. Jones[ab]; L. Lue[a]; A. P. Ormerod[c]; G. J. T. Tiddy[a]
[a] School of Chemical Engineering & Analytical Science, University of Manchester, Manchester, UK [b] Biopharmaceutics Research & Development, Bristol-Myers-Squibb, Moreton, Wirral, UK [c] Unilever Research & Development, Sharnbrook, Bedfordshire, UK

To cite this Article Jones, J. W. , Lue, L. , Ormerod, A. P. and Tiddy, G. J. T.(2010) 'The influence of sodium chloride on the self-association and chromonic mesophase formation of Edicol Sunset Yellow', Liquid Crystals, 37: 6, 711 — 722
To link to this Article: DOI: 10.1080/02678292.2010.486174
URL: http://dx.doi.org/10.1080/02678292.2010.486174

Liquid Crystals,
Vol. 37, Nos. 6–7, June–July 2010, 711–722

Taylor & Francis
Taylor & Francis Group

INVITED ARTICLE

The influence of sodium chloride on the self-association and chromonic mesophase formation of Edicol Sunset Yellow

J.W. Jones[a,b]*, L. Lue[a], A.P. Ormerod[c] and G.J.T. Tiddy[a]*

[a]*School of Chemical Engineering & Analytical Science, University of Manchester, Manchester, UK;* [b]*Biopharmaceutics Research & Development, Bristol-Myers-Squibb, Moreton, Wirral, UK;* [c]*Unilever Research & Development, Sharnbrook, Bedfordshire, UK*

(*Received 17 December 2009; accepted 31 March 2010*)

We have investigated the effect of an inorganic electrolyte (sodium chloride) on the aggregation behaviour and liquid crystals of Edicol Sunset Yellow. Edicol self-aggregates in aqueous solution to form single molecule stacks, which then become ordered to form nematic and hexagonal (columnar) mesophases at high concentrations. We have employed changes in the ^{1}H nuclear magnetic resonance (NMR) chemical shifts to monitor the aggregate formation in solution. A single spectrum is observed at all concentrations because the exchange between Edicol monomers in solution and those in stacks is fast on the NMR time scale. The results show that at low Edicol concentrations (<1 wt%) the concentration of aggregates is small, but at high concentrations (20 wt%) the fraction of monomers is tiny. At low Edicol concentrations, low levels of salinity appear to alter aggregate shape and size, resulting in a disaggregation/aggregation effect occurring over four orders of magnitude of added electrolyte. However, little alteration is seen in the fraction of aggregates. At high electrolyte levels, when the Debye length is comparable to the stack lengths (a few nanometres), the fraction of aggregates increases, presumably because of the reduced intra-stack electrostatic repulsion. Importantly, we have also shown that the isodesmic theory of aggregation (equal *K*) is too simple to describe accurately the aggregation process from the monomer to the pre-nematic phase concentrations. NMR quadrupole splittings indicate that there is no specific Na^+ ion binding to the stacks. At the very highest concentrations of Edicol and sodium chloride the aggregates and mesophases are destabilised. The reason for this has yet to be elucidated.

Keywords: chromonic; aggregation; isodesmic; Edicol Sunset Yellow; salt; sodium chloride; NMR; chemical shift; quadrupole

1. Introduction

Chromonic liquid crystals are formed by compounds with multi-aromatic rings that also have polar substituents [1]. The compounds self-aggregate in dilute aqueous solution; then, when the concentration of aggregates (stacks) is sufficiently high, these aggregates become ordered to form mesophases; see Figure 1 [2, 3]. Whilst chromonic mesophases have been known for many years (for a summary see Collings and Dickinson [4]), they remain mysterious. Alfred Saupe was the first to examine the systems using nuclear magnetic resonance (NMR) [5], at the same time that he made significant contributions to the study of surfactant nematic phases. His group identified two different amphiphilic nematic phases formed from rod and disc micelles. However, the most remarkable discovery was a third amphiphilic nematic phase which was biaxial [6]. Biaxial nematics have been well-established in lyotropic systems since that time. One of us (GJTT) is particularly grateful for instructive discussions on surfactant mesophases and their properties where Saupe had particular insights. One example is in considering the flexibility of rod-like micelles with an elliptical cross-section. As Saupe pointed out, the easy-bending mode is around the short axis, the opposite of the common assumption. The present paper continues the theme of NMR studies on chromonics.

The mechanism of aggregation for chromonic systems has been considered several times before [7–14] and is often assumed to be isodesmic in nature, i.e. the energy of adding or indeed removing an individual molecule from an aggregate stack is independent of the stack size. We suspect that the aggregation behaviour of Edicol Sunset Yellow (see Figure 1), a commonly studied dye, is more complex than that described by an isodesmic model. To investigate this we have used ^{1}H high-resolution NMR to measure the chemical shifts, δ, of Edicol as a function of concentration. The ring current shielding effect of the aromatic compounds induces relatively large changes in the chemical shifts of neighbouring molecules in the same stack. As the exchange of monomers and molecules in the stacks is very fast on the NMR time scale, the measured chemical shift is a weighted average of

---

*Corresponding authors. Email: john.jones@bms.com; gordon.tiddy@manchester.ac.uk

ISSN 0267-8292 print/ISSN 1366-5855 online

DOI: 10.1080/02678292.2010.486174
http://www.informaworld.com

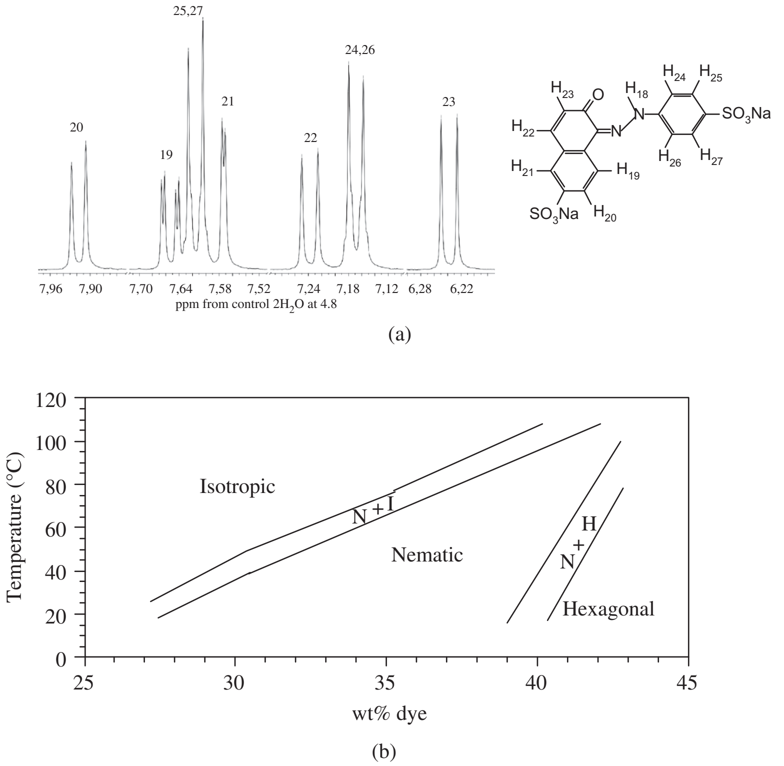

(a)

(b)

Figure 1. (a) ^{1}H NMR spectrum of Edicol in aqueous solution (1 wt%) at 22°C together with the assignments (δ values referenced to ^{1}HOD at 4.8000 ppm [16]). (b) The phase diagram of aqueous Edicol Sunset Yellow [2, 3], taken with permission.

the free and complexed molecules [2, 9, 10]. Since the monomer chemical shift is expected to be independent of concentration, changes in chemical shifts can be attributed to changes in the relative populations of monomers and aggregates.

Edicol has two possible tautomeric forms, but we have previously shown that the azo tautomer (see Figure 1) is the one present [2] and that it aggregates to form single molecule stacks in solution both in the nematic and hexagonal phases [2, 3, 13, 15]. Figure 1 shows a typical NMR spectrum with proton assignments for Edicol at pre-liquid crystal concentrations. In this study we follow the aggregation of Edicol by measuring the changes in the proton chemical shifts. It must be noted that the assignments of protons H_{19} and H_{20} differ from those given in our previous paper [2], where due to an error they were transposed in the structure given.

We have previously shown that changes in chemical shifts can be combined with other data to determine the structure of the aggregates and their repeat/unit structure [2]. We now aim to investigate the detailed aggregation mechanism in water and salt solutions using the chemical shifts. Edicol is a di-anionic compound; hence we can expect that electrostatic repulsions due to the ionised sulphonate groups will act to prevent aggregation. This repulsion is expected to be reduced by the addition of an electrolyte [15, 17–19]. Thus we have measured the δ values as a function of both the Edicol and electrolyte concentrations of sodium chloride.

2. Experimental section

2.1 Materials

Edicol Sunset Yellow (M_w 452.37 g mol^{-1}) was purified via high-performance liquid chromatography (HPLC) using the method described in our previous paper [2] and then stored in a desiccator. The heavy water (99.8% ^{2}H) and sodium chloride (M_w 58.44 g mol^{-1}) were purchased from Sigma-Aldrich and used without further purification.

2.2 Methods

Samples were prepared at specific concentrations using heavy water and then vortexed at elevated temperatures before cooling back to room temperature. After one day the NMR spectra were measured using a Bruker 400 MHz spectrometer at 295 ± 0.5 K with the use of a temperature-controlled air stream.

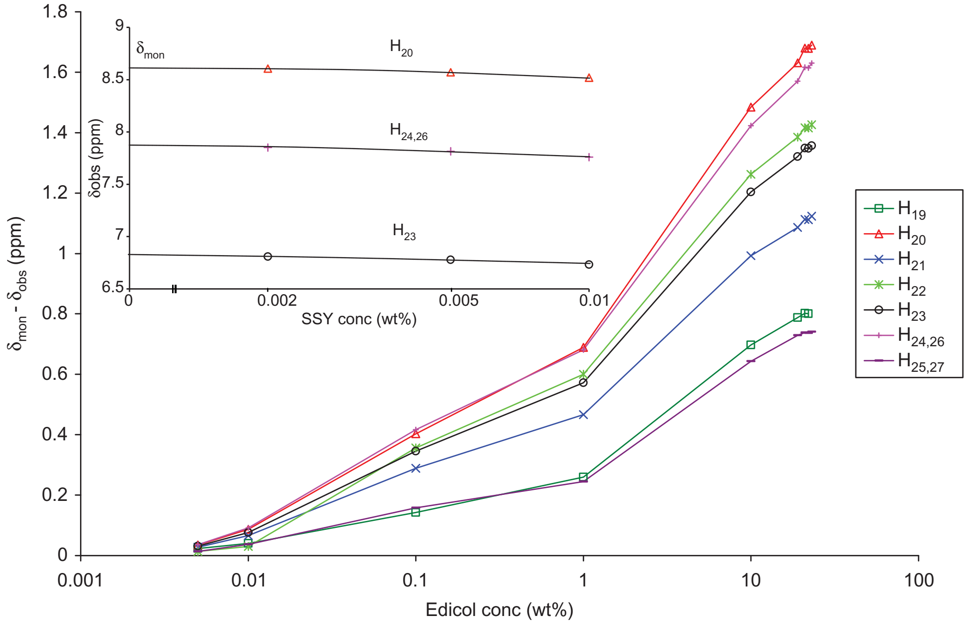

Figure 2. The chemical shifts of pure Edicol relative to the monomer chemical shift at 22°C (δ_{mon}). Value fitted using the isodesmic model and an equilibrium constant, K, of 340 m^{-1} (for further discussion see later). Note that m denotes the molality which is the number of moles of solute per kilogram of solvent (colour version online).

The δ-values were measured using the ^{1}HOD peak as a reference ($\delta = 4.800$ ppm) [16]. Sodium chloride and ^2H_2O were mixed at several different molarities, to which the Edicol was then added.

3. Results and discussion

3.1 The aggregation behaviour of Edicol

In our previous study we used the change in chemical shifts, δ_{obs}, with concentration to follow the behaviour of Edicol [2]. Here, we report a more extensive study of δ_{obs} as a function of concentration to examine the aggregation process in more detail. Various models have been developed to describe this, the most common being the isodesmic model. For all of these models we assume that the chemical shift changes result from aggregation and that δ_{obs} is invariant at very low concentrations, giving the monomer chemical shift, δ_{mon}; we also assume that δ_{obs} is invariant at concentrations close to the nematic/isotropic phase boundary, giving the chemical shift δ_{agg}. As shown in Figure 2 (inset), at the lowest concentrations measured there are still small changes in δ_{obs}. The values of δ_{mon} have been estimated using the isodesmic model (see later). To highlight changes in δ, we report the change in δ_{obs} relative to the monomer chemical shift δ_{mon}, as shown in Figure 2. This figure includes data for more samples than previously reported [2]. The results are also listed in Table 1.

The trend in chemical shift associated with the aggregation follows an S-shaped curve, which can be approximated into three different regions. The first region exists at low Edicol concentrations below 0.01 wt% at which the change in δ_{obs} is small and little aggregation is observed. The second region lies between 0.01 wt% and 19 wt% during which there is a significant increase in δ and molecular aggregation. The final region lies at Edicol concentrations greater than 19 wt%, and is typified by a decrease in the change of δ.

3.2 Fitting the isodesmic model

Current schools of thought argue for the case of an isodesmic model of only one constant value and two limiting chemical shifts δ_{mon} and δ_{agg}. Previous published papers have proved this to be the case, with both the monomer–dimer and isodesmic model being successfully applied to the aggregation behaviour of several aromatic ring molecules [8, 14, 20], including the dye Orange II [9, 21]. Several reviews have been published regarding different models covering the aggregation from simple benzene molecules to squaraine dyes, so only a brief précis will be given here [7, 8]. The aggregation of chromonic molecules can be approximated as a stepwise reaction, monomer to dimer to trimer etc. to stack:

Table 1. ^{1}H chemical shifts, δ_{obs}, of Edicol in $2H_2O$ at 22°C.

	H_{19}		H_{20}		H_{21}		H_{22}		H_{23}		$H_{24,26}$		$H_{25,27}$		
Conc. wt%	$\delta_{mon}-$ δ_{obs}	%[a]	$\delta_{mon}-$ δ_{obs}	%	$\delta_{mon}-$ δ_{obs}	%	$\delta_{mon}-$ δ_{obs}	%	$\delta_{mon}-$ δ_{obs}	%	$\delta_{mon}-$ δ_{obs}	%	$\delta_{mon}-$ δ_{obs}	%	wt% mon[d]
δ_{mon}[b]	7.917		8.630		8.045		7.841		6.820		7.867		7.882		
0.002	0.004	0.49	0.019	1.11	0.006	0.49	0.002	0.17	0.011	0.78	0.017	1.01	0.004	0.52	0.002
0.005	0.027	3.38	0.054	3.18	0.032	2.86	0.016	1.11	0.042	3.03	0.053	3.20	0.018	2.36	0.005
0.01	0.044	5.44	0.106	6.22	0.072	6.35	0.033	2.31	0.087	6.34	0.108	6.56	0.041	5.49	0.009
0.1	0.146	18.2	0.422	24.7	0.294	26.1	0.359	25.1	0.356	26.0	0.434	26.3	0.162	21.8	0.074
1	0.264	32.8	0.708	41.4	0.472	41.8	0.603	42.2	0.582	42.6	0.698	42.4	0.249	33.4	0.58
10	0.701	87.1	1.503	87.9	0.998	88.6	1.264	88.5	1.215	88.8	1.440	87.4	0.647	86.9	1.2
19	0.791	98.4	1.650	96.6	1.092	96.8	1.388	97.1	1.332	97.4	1.588	96.4	0.733	98.5	0.57
21	0.806	100	1.699	99.4	1.119	99.1	1.419	99.3	1.360	99.4	1.633	99.2	0.742	99.6	0.13
22	0.804	100	1.698	99.4	1.118	99.0	1.418	99.2	1.359	99.3	1.632	99.1	0.741	99.5	0.15
23	c	–	1.709	100	1.129	100	1.429	100	1.368	100	1.647	100	0.745	100	–
τ_c^S/ns mon			0.93						0.4				1.1		
τ_c^S/ns agg[d]			39						37				38		

Notes: [a] %= $(\delta_{mon}-\delta_{obs})/(\delta_{mon}-\delta_{agg})$, a linear relationship. [b]Extrapolated value. [c]Very weak, very broad peak thus unable to estimate chemical shift. [d]Calculated from H_{20}, H_{23}, $H_{24,26}$. δ_{agg} is assumed to be the chemical shift at the final concentration close to the phase boundary between the isotropic and nematic phases. Note: These values are slightly different from our previous publication because of different sample batches and purification; we believe this to be our purest sample [2].

$$A_1 + A_1 \overset{K_2}{\Leftrightarrow} A_2 \qquad [A_2] = K_2[A_1]^2, \tag{1}$$

$$A_2 + A_1 \overset{K_3}{\Leftrightarrow} A_3 \qquad [A_3] = K_3[A_1]\cdot[A_2] = K_2K_3[A_1]^2, \tag{2}$$

$$A_{n-1} + A_1 \overset{K_n}{\Leftrightarrow} A_n \qquad [A_n] = K_n[A_{n-1}]\cdot[A_1]. \tag{3}$$

Here K_2, K_3 and K_n are the equilibrium constants for the addition of a monomer to a monomer, dimer and $(n-1)$ – mer respectively, and $[A_1]$, $[A_2]$, $[A_3]$, …. $[A_n]$ are the molar concentrations of the monomer, dimer, trimer and n-mer species, respectively. The isodesmic (equal model) assumes that for all aggregation events (monomer to dimer to stack) the equilibrium constants are equal, i.e. $K = K_1 = K_2 = K_3 = \ldots = K_n$. Thus, for chemical shift data the equal K process can be written as

$$\Delta = \delta_{obs} - \delta_{mon} = \left(\delta_{agg} - \delta_{mon}\right)Kc_1, \tag{4}$$

where δ_{obs} is the observed ^{1}H chemical shift, δ_{mon} and δ_{agg} are the chemical shifts of the monomer and aggregated species, respectively, and $c_1 = [A_1]$. As has been shown previously (Martin [7]; Chen *et al.* [8]), c_1 is related to c_T, the total concentration, by

$$Kc_T = Kc_1 \Big/ (1 - Kc_1)^2. \tag{5}$$

The solution of which leads to a term for Kc_1:

$$Kc_1 = \frac{2Kc_T + 1 - \sqrt{4Kc_T + 1}}{2Kc_T}. \tag{6}$$

Thus, if the experimental data follow isodesmic aggregation, a simple plot of δ_{obs} against log c_T should follow the theoretically calculated values fitted by estimating K and δ_{agg}. It is important to note that the fitting of Equation (4) is typically carried out by linear regression and is heavily reliant on both the parameters, K and δ_{agg}. This can result in the production of a wide range of K values between different experimental techniques. We have reduced the number of variables by subdividing $\delta_{obs} - \delta_{agg}\big|_{c_T}$ (the chemical shift measured at the concentration C_T) by $\delta_{obs} - \delta_{agg}\big|_{c_{max}}$ (the chemical shift at the maximum measured concentration) (see Equation (7)), thus reducing the number of variables, facilitating the preliminary fitting of only K and later δ_{agg} by minimising the error between the theoretical and experimental results:

$$Kc_1(c_T) \Big/ Kc_1(c_{max}) = (\delta - \delta_{mon})\big|_{c_T} \Big/ (\delta - \delta_{mon})\big|_{c_{max}}. \tag{7}$$

Figure 3 shows our solution of fitting the isodesmic model to the experimental data of protons H_{19}, H_{23} and $H_{24,26}$. We have weighted the data to fit both monomer and aggregate concentrations by preferentially minimising the error in the said region. Details are summarised in Table 2.

We have found that in using the isodesmic model it is possible to approximate behaviour at very low

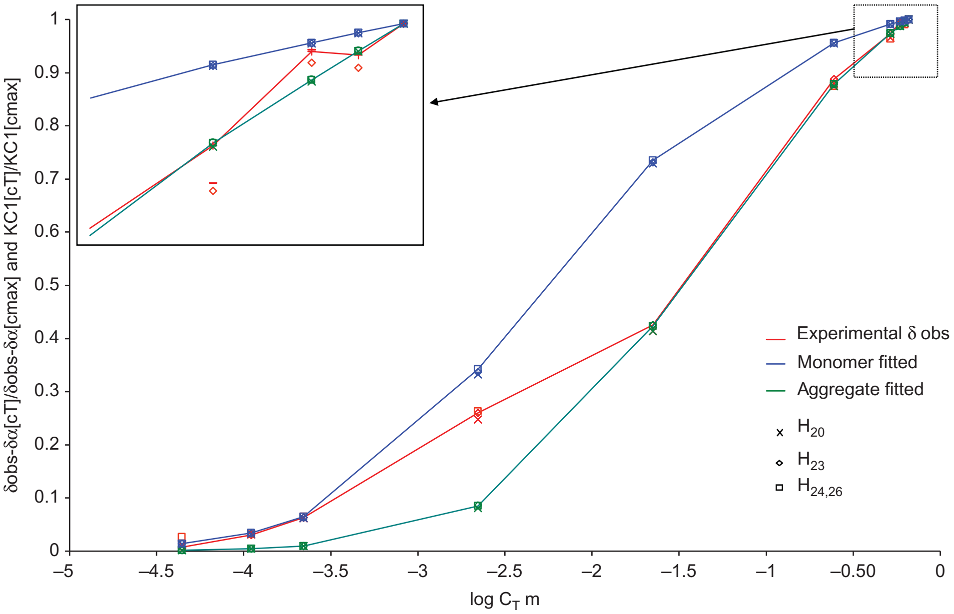

Figure 3. Modelling the aggregation behaviour of pure Edicol as a function of concentration using the isodesmic model [7, 8, 10] (colour version online).

Table 2. Aggregation parameters (K, δ_{agg}) of Edicol in aqueous solution at 22°C fitted using the isodesmic model.

		Close to N phase		Close to monomer	
Proton	δ_{mon}/ppm	K/m^{-1}	δ_{agg}/ppm	K/m^{-1}	δ_{agg}/ppm
H_{20}	8.625	34.1	6.517	312	6.794
H_{23}	6.820	36.6	5.144	301	5.352
$H_{24,26}$	7.867	36.1	5.854	311	6.101

(ca. 10^{-5} m) and high (0.7 m) concentrations. The isodesmic model returns what can be considered reasonable values for K and δ_{agg} (as shown in Table 2) [2, 3, 7]. However, Figure 3 does reveal significant deviations between the fitted model and experimental data over a wide range of concentrations ca. 10^{-3} and 0.5 m, thus revealing that the equal K model does not hold for Edicol Sunset Yellow. This conclusion is in agreement with a recent X-ray study of the Edicol liquid crystal phases by Joshi *et al.* [22].

Moreover, there are also some short comings in the assumption that a single value of δ_{agg} is sufficient for all concentrations. Table 1 shows the percentage of Edicol in aggregates at each concentration, calculated from δ_{obs} for each separate proton signal. At each concentration this should be the same for all the protons; it clearly is not! At the lowest concentration, the calculated fraction of aggregates falls in the range 0.17–1.11 wt%. For the high concentrations (≥10 wt%) all the proton shifts give similar values for the fractions of aggregates. However, for 0.002–1.0 wt% the values for H_{19}, H_{22} and $H_{25,27}$ are generally smaller than for the other protons. It does not seem likely that the values of δ_{agg} could be very much larger than the values given for H_{20} and $H_{24,26}$. Thus, at the lower concentrations, the values of δ_{agg} for H_{19}, H_{22} and $H_{25,27}$ are smaller than the estimated values. We conclude that there is a change in the structure of the aggregates with increasing concentration, with the aggregates probably becoming more compact at higher concentrations. (Note that in the mesophases the separation between the aggregates is of the same order as the longest Edicol dimension.) It is not immediately clear what structural changes would lead to the observed shift patterns, but if the single aromatic ring was not fully incorporated into the stacks at low concentrations this would give the smaller shifts for $H_{24,26}$. At higher concentrations the crowding of the stacks would lead to more compact packing and a larger shift. This change in aggregate structure would lead to non-isodesmic behaviour.

The final column of Table 1 lists the monomer concentration calculated by subtracting the concentration of Edicol in aggregates from the total concentration. This shows a maximum at ca. 10 wt%, above which the monomer concentration decreases. Whilst the exact monomer level calculated does depend on the value taken for δ_{agg}, this overall picture follows directly from the assumption that $\delta = \delta_{agg}$ at some high concentration. However, this assumption does not allow the identification of the concentration at which the number of monomers starts to decrease. Note that the monomer concentration is not related directly to the Edicol chemical potential at high concentrations. This will increase monotonically across the whole concentration range.

We should also add a cautionary note concerning the use of the two-state model to analyse the concentration dependence of the chemical shifts. In particular, the molecules at the ends of the stacks will have a different chemical shift from those fully inside the stacks. Thus we do not expect the small aggregates (e.g. dimers, trimers) to have the same δ_{agg} as larger aggregates; their values are likely to be closer to δ_{mon} by, say, 0.4 ppm or so. However, the expected concentrations of these species are smaller than that of the monomer. Hence this will alter the values in Table 1 to some extent, but it does not alter the overall picture. The maximum in the monomer concentration is still present, and hence the behaviour is non-isodesmic, at least above ca. 10–15 wt%.

3.3 The aggregation behaviour of Edicol in sodium chloride solutions

Inorganic electrolytes have been shown to have a significant effect on the phase behaviour of liquid crystalline Edicol, generally increasing the stability of the mesophases [3, 15, 17–19]. Mostly these authors have studied a single Edicol concentration and varied the electrolyte level. Park *et al.* [15] report an increase in the mesophase transition temperatures at 0.9 m Edicol with a range of salt levels. The increase varies from ca. 2°C at 0.3 m salt to 5°C at 1.2 m. Figure 4 shows the phase boundaries for Edicol in 1 m NaCl compared with the behaviour in water, over a range of concentrations. Note that these results were obtained using a slightly less pure Edicol sample than that employed for the phase diagram in [11], although impurity peaks present in the proton NMR spectra were of low intensity (<1 wt%). The phase transitions are known to differ by a few degrees for different batches [9, 11, 13], but the overall behaviour is generally similar. This addition of electrolyte results in a slight destabilisation of the nematic phase at the highest concentrations. There is also a significant shift to higher concentrations for the nematic phase, while the hexagonal phase occurs at even higher concentrations. These changes are in the opposite direction from those reported by Park *et al.* [15] and others. However, we note that the measurements of Park *et al.* [15] were made on a sample with 28.9 wt% Edicol, whereas our measurements start at ca. 33 wt%. There appears to be a crossover in behaviour at this point which requires further measurements. The shift in the nematic/hexagonal boundaries above 33% is consistent with a decrease in mesophase stability, with the less ordered nematic phase persisting to higher concentrations.

It has been suggested that these phenomena are a direct consequence of electrostatic charge screening due to the presence of the NaCl and are related to both the valency of the counterion and, to some extent, its concentration [15, 18]. A well-established method to monitor ion binding in surfactant liquid crystals is to measure the ^{23}Na quadrupolar splittings (ΔNa) [2, 23, 24]. We have made measurements on liquid crystalline phases containing Edicol, where the ΔNa values fall in the range 3.2–3.7 kHz, showing little variation with concentration and only a small decrease with increasing temperature [2]. From this we concluded that they followed a similar pattern to that for ionic surfactant mesophases, where the ion-condensation hypothesis often applies [25]. For highly charged aggregates such as Edicol stacks (and micelles

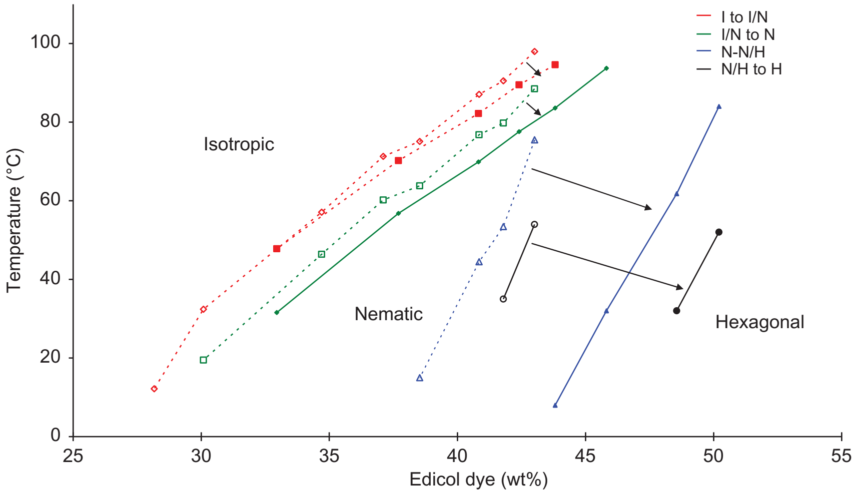

Figure 4. A phase diagram showing Edicol Sunset Yellow in 1 m NaCl solution (solid line) in comparison to aqueous Edicol (dashed line) (colour version online).

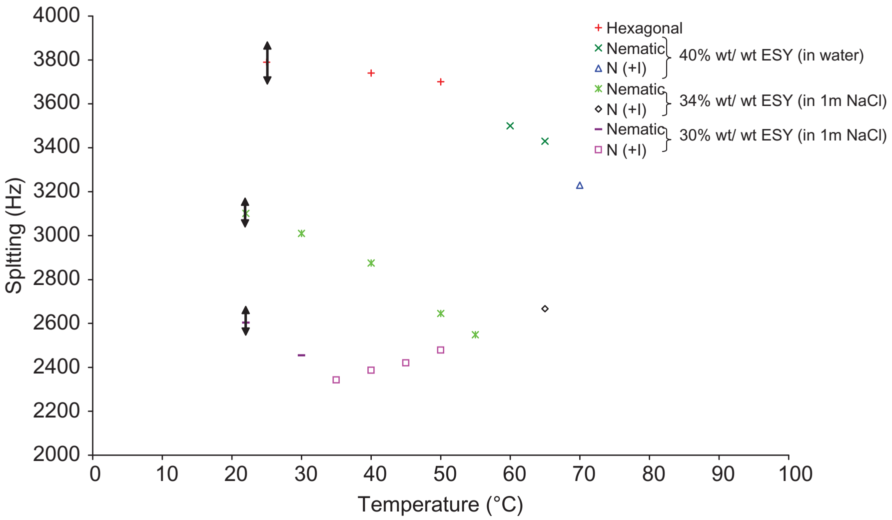

Figure 5. The ^{23}Na quadrupolar splittings of Edicol in 1 m NaCl as a function of temperature (colour version online).

of ionic surfactants) the counter-ions condense onto the charged surface to neutralise 70–80%, say, of the charges. The remaining ions form a diffuse double layer. Thus alterations in aggregate concentration do not greatly alter the ion binding. Because the ΔNa values are determined by the fraction of Na^+ ions at the aggregate surface, these are also fairly invariant with composition. Values for Edicol with 1 m sodium chloride are given in Figure 4. The added NaCl reduces the ΔNa values from within the range 3.2–3.7 kHz to the range 2.3–3.0 kHz. We can assume that the added electrolyte has a zero ΔNa value if added Na^+ is not binding to the aggregates, but simply increases the total concentration of sodium ions present. Then we calculate a range for ΔNa in the presence of salt of 2.0–2.7 kHz from the results for the salt-free system. This is very close to the actual values observed, giving firm evidence against any role of specific ion binding from the added electrolyte for this case.

From a comparison of the concentrations at which mesophases form, the effect of NaCl on the molecular aggregation behaviour of Edicol is not clear. With this in mind, we have examined in detail the aggregation behaviour of Edicol in solutions of NaCl over a wide range of concentrations using proton NMR. The results are given in Figure 5 and Table 3. To emphasise the influence of the electrolyte, the data in Figure 6 are given at constant Edicol concentration and varying sodium chloride concentration. The data are analysed using the two-state model (monomers/aggregates) and hence, as with the data for the salt-free system, we neglect any change in δ_{agg} with aggregate size.

The results in Figure 5 and Table 3 reveal several interesting points regarding the effect of NaCl on Edicol aggregation behaviour. As with the pure Edicol systems, the trend can be split into distinct regions. The first region bounds a range of four orders of magnitude (10^{-5}–10^{-2} M NaCl) within which a cursory observation reveals a negligible change in δ_{obs}. Contrary to this initial observation, closer inspection reveals that δ_{obs} is not constant; rather it varies significantly from one concentration to another in a see-saw fashion. This variation is reproducible with several repeated samples. Remarkably, this suggests that the monomer/aggregate equilibrium is affected by small and varying amounts of NaCl, sometimes resulting in a small amount of disaggregation. This phenomenon persists until the NaCl concentration reaches 10^{-1} M, at which point a sharp increase in the aggregation is observed (continuing up to and including 3 M NaCl); a trend which defines the second region. Throughout this range of concentration, aggregation gradually increases, the sharp gradient change corresponding to a fractional increase from 0.07 to 0.4 (from 10^{-2} to 10^{-1} M) in the number of aggregates in comparison to the pure Edicol system (0.01 wt%). It must be noted that this trend is evident in each of the four Edicol concentrations shown in Figure 4, but decreases in magnitude with Edicol concentration (e.g. a change in $\delta_{\mathrm{mon}} - \delta_{\mathrm{obs}} = 0.9, 0.8, 0.6, 0.2$ for 0.01, 0.1, 1 and 10 wt% Edicol, respectively) suggesting that NaCl is more effective for larger aggregates [15]. Coincidentally, it is at this same concentration that aggregation of Edicol is encouraged by NaCl, suggestive of a critical concentration. Thus, it can be argued that the addition of excess Na^+ ions screens the repulsive interaction between opposing Edicol molecules facilitating the aggregation of *n*-mers at lower Edicol concentrations. This would then suggest that the size

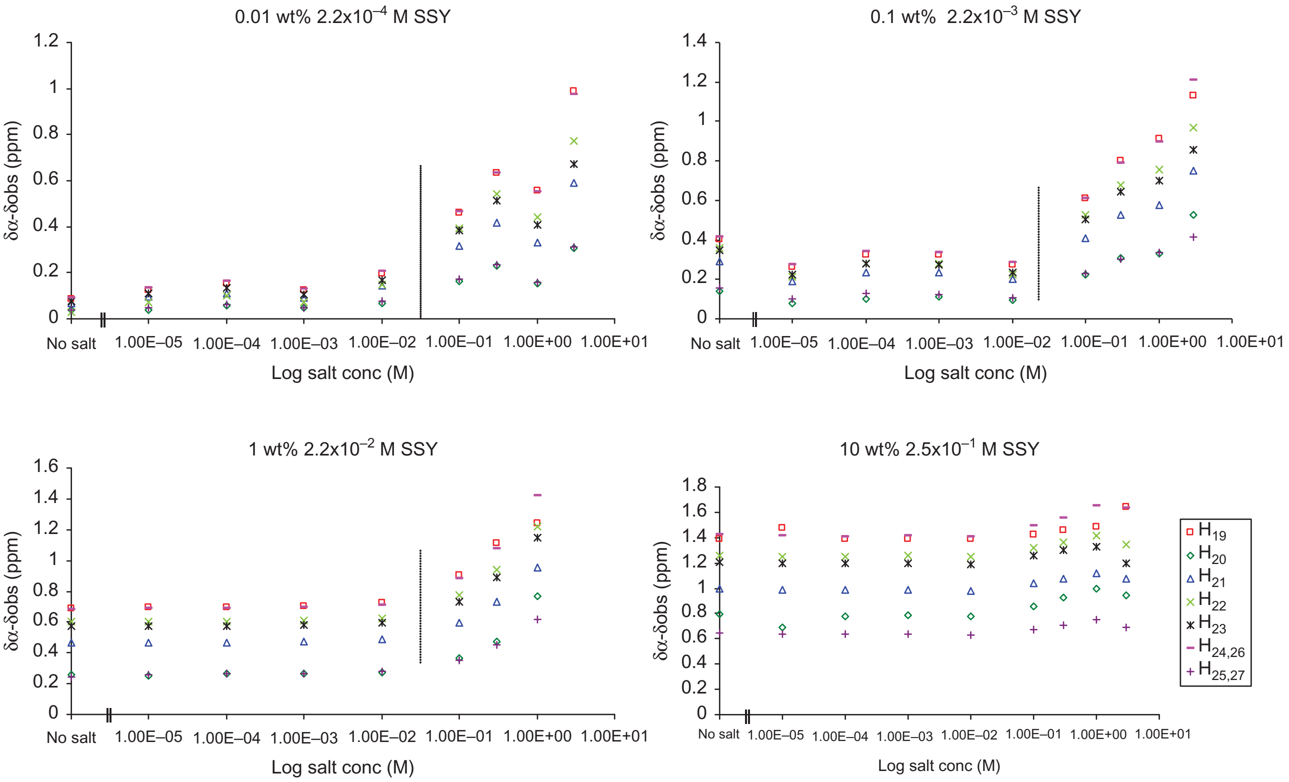

Figure 6. The effect of NaCl on the observed chemical shift, δ_{obs}, relative to that at the monomer concentration, δ_{mon}, of Edicol at 22°C. The dashed line indicates a significant change in gradient and aggregation of the Edicol molecules (colour version online).

of Edicol aggregates is limited by the electrostatic repulsions.

Table 3 lists the fraction of Edicol in aggregates calculated from the data for each proton separately. Because of the very broad lines for the high concentration spectra (20 wt%) with high electrolyte levels we have taken the values of δ_{agg} to be those for the 10 wt% samples. This will result in an overestimation of the monomer concentration. However, even so, it can be seen that the monomer concentration decreases monotonically as the sodium chloride concentration increases. The sharp decrease in monomer concentration at 0.1 M electrolyte and above could lead to a small increase (ca. 1 wt%) in the volume fraction of aggregates, which might account for the increase in mesophase stability at intermediate electrolyte levels as reported by Park *et al.* [15].

We have fitted the data at all concentrations using the isodesmic model. The fit is poor, but the values of K are listed in Table 4. These increase strongly with electrolyte concentration as expected.

Importantly, further information on the aggregate size can be gleaned from the NMR spectra, through using the transverse relaxation time (T_2) and, thus, the correlation time, τ_c, the results of which are detailed in the following section.

3.4 Correlation time, τ_c, and stack length

We have estimated the Edicol stack size by calculating the ^{1}H transverse spin relaxation times, T_2, from the half-height width of the peaks, $\Delta\nu_{1/2}$, in the chemical shift spectra using the relation $(\pi T_2)^{-1} = \Delta\nu_{1/2}$. To achieve this, we assume that the Edicol mobility can be described by two correlation times previously used for micelles [2]. In micelles, the first is a slow motion due to the orientation of the molecule at the micelle/water interface, τ_c^S, and the second a fast motion due to local rotation, translation and conformational changes, τ_c^F. In this work we assume that the maximum value of the τ_c^F term occurs for the narrowest peaks [26]. Thus T_2 is found from

$$\begin{aligned}\frac{1}{T_2} &= \frac{9}{8}\frac{\gamma^4\hbar^2}{r^{6c}}\left[S^2 g\left(\tau_c^S\right) + \left(1-S^2\right)5\tau_c^F\right]g(\tau_c)\\ &= \frac{3}{2}\tau_c + \frac{5}{2}\frac{\tau_c}{1+\omega_0^2\tau_c^2} + \frac{\tau_c}{1+4\omega_0^2\tau_c^2},\end{aligned} \qquad (8)$$

where γ is the nuclear gyromagnetic ratio and S is the orientational order parameter, which we take as 0.6 from our previous work [2].

Note that the measurement of $\Delta\nu_{1/2}$ is complicated by the influence of scalar J coupling between the aromatic protons which splits the resonances into multiple peaks. At low concentrations the individual peaks

Table 3. ^{1}H chemical shifts of Edicol and aggregation parameters in NaCl solutions of various strengths at 22°C.

	H_{19}		H_{20}		H_{21}		H_{22}		H_{23}		$H_{24,26}$		$H_{25,27}$		
Conc. **(NaCl)** wt%	$\delta_{mon} - \delta_{obs}$	%^{a}	$\delta_{mon} - \delta_{obs}$	%	$\delta_{mon} - \delta_{obs}$	%	$\delta_{mon} - \delta_{obs}$	%	$\delta_{mon} - \delta_{obs}$	%	$\delta_{mon} - \delta_{obs}$	%	$\delta_{mon} - \delta_{obs}$	%	wt% mon^c
$\delta_{mon}{}^b$ (ppm)	7.917		8.625		8.04		7.841		6.820		7.867		7.882		
No salt															
0.01	0.044	5.52	0.106	6.44	0.072	6.57	0.033	2.38	0.087	6.51	0.108	6.80	0.041	5.58	0.009
0.1	0.146	18.5	0.422	25.6	0.294	26.9	0.359	25.9	0.356	26.7	0.434	27.3	0.162	22.1	0.074
1	0.264	33.3	0.708	42.9	0.472	43.2	0.603	43.5	0.582	43.7	0.698	43.9	0.249	33.9	0.56
10	0.701	88.5	1.503	91.1	0.998	91.4	1.264	91.1	1.215	91.2	1.440	90.7	0.647	88.2	0.9
19	0.791	100	1.650	100	1.092	100	1.388	100	1.332	100	1.588	100	0.733	100	–
1x10^{-5} M															
0.01	0.041	5.20	0.146	8.57	0.099	8.86	0.076	5.37	0.120	8.81	0.150	9.21	0.053	7.08	0.009
0.1	0.082	10.6	0.279	16.4	0.196	17.5	0.217	15.3	0.235	17.3	0.290	17.8	0.104	14.0	0.083
1	0.253	32.5	0.713	41.9	0.472	42.2	0.606	42.7	0.583	42.9	0.702	43.1	0.266	35.7	0.57
10	0.691	88.7	1.493	87.8	0.989	88.3	1.254	88.5	1.205	88.7	1.429	87.7	0.639	85.8	1.2
20	0.779	100	1.700	100	1.120	100	1.417	100	1.358	100	1.631	100	0.744	100	–
1x10^{-4} M															
0.01	0.061	8.76	0.173	11.6	0.118	11.9	0.105	8.38	0.144	11.9	0.179	12.5	0.065	10.2	0.009
0.1	0.106	15.2	0.346	23.2	0.241	24.4	0.285	22.7	0.292	24.3	0.358	25.1	0.132	20.6	0.076
1	0.267	38.1	0.713	47.9	0.475	48.1	0.608	48.5	0.587	48.8	0.703	49.3	0.269	42.2	0.51
10	0.700	100	1.491	100	0.989	100	1.253	100	1.204	100	1.428	100	0.639	100	–
1x10^{-3} M															
0.01	0.050	7.14	0.143	9.55	0.096	9.71	0.073	5.8	0.118	9.78	0.147	10.3	0.053	8.28	0.009
0.1	0.119	16.9	0.342	22.8	0.236	23.8	0.280	22.2	0.288	23.8	0.353	24.6	0.129	20.1	0.076
1	0.270	38.4	0.723	48.2	0.481	48.4	0.615	48.8	0.594	49.1	0.712	49.6	0.272	42.4	0.51
10	0.704	100	1.499	100	0.993	100	1.259	100	1.210	100	1.435	100	0.642	100	–
1x10^{-2} M															
0.01	0.073	10.5	0.217	14.6	0.151	15.3	0.151	12.1	0.180	15.0	0.224	15.7	0.081	12.7	0.009
0.1	0.098	13.9	0.292	19.7	0.205	20.8	0.228	18.2	0.244	20.4	0.302	21.2	0.110	17.3	0.08
1	0.280	40.2	0.742	49.9	0.492	49.9	0.630	50.5	0.608	50.7	0.730	51.2	0.281	44.1	0.5
10	0.697	100	1.487	100	0.985	100	1.249	100	1.200	100	1.424	100	0.636	100	–
0.1 M															
0.01	0.166	22.5	0.482	30.7	0.321	30.8	0.397	30.1	0.393	31.	0.484	32.1	0.176	25.8	0.007
0.1	0.228	31.0	0.631	40.2	0.417	39.9	0.529	40.1	0.513	40.6	0.626	41.6	0.234	34.4	0.06
1	0.368	49.9	0.922	58.7	0.604	57.9	0.775	58.8	0.745	58.9	0.898	59.6	0.358	52.5	0.41
10	0.737	100	1.571	100	1.042	100	1.319	100	1.265	100	1.507	100	0.681	100	–
0.3 M															
0.01	0.235	30.5	0.651	39.7	0.425	39.3	0.543	39.6	0.524	39.9	0.653	41.4	0.238	33.3	0.006
0.1	0.312	40.5	0.821	50.1	0.53	48.9	0.681	49.7	0.653	49.8	0.805	51.1	0.308	43.1	0.05
1	0.478	62.0	1.128	68.8	0.735	67.9	0.943	68.9	0.901	68.7	1.096	69.6	0.453	63.4	0.31
10	0.771	100	1.638	100	1.082	100	1.370	100	1.311	100	1.575	100	0.715	100	–
1 M															
0.01	0.182	22.9	0.625	36.6	0.337	29.9	0.478	33.7	0.450	33.5	0.601	36.0	0.190	25.1	0.007
0.1	0.336	42.4	0.930	54.5	0.584	51.9	0.756	53.4	0.709	52.8	0.915	54.9	0.338	44.7	0.047
1	0.553	69.8	1.481	86.9	0.961	85.4	1.225	86.5	1.158	86.3	1.439	86.4	0.624	82.5	0.14
10	0.792	100	1.705	100	1.125	100	1.416	100	1.342	100	1.666	100	0.756	100	–
3 M															
0.01	0.312	32.8	1.01	60.9	0.597	55.3	0.775	57.7	0.683	56.4	0.99	59.9	0.318	45.7	0.004
0.1	0.53	55.7	1.149	69.3	0.754	69.9	0.973	72.4	0.869	71.7	1.225	74.0	0.438	63.0	0.028
1	–	–	–	–	–	–	–	–	–	–	–	–	–		
10	0.951	100	1.659	100	1.079	100	1.344	100	1.211	100	1.654	100	0.695	100	–

Notes: ^{a} %= (δ_{mon}– δ_{obs})/(δ_{mon}– δ_{agg}), a linear relationship. ^{b}We assume δ_{mon} to be the same in both aqueous and NaCl systems. ^{c} Calculated from H_{20}, H_{23}, $H_{24,26}$. Note: The effect of NaCl at low molar concentrations, i.e. 10^{-4}, 10^{-3} and 10^{-2}, is real and reproducible.

can be distinguished, so it is easy to measure $\Delta\nu_{1/2}$. As the lines become broadened, there is overlapping of adjacent resonances and the values of $\Delta\nu_{1/2}$ are overestimated. In these cases we have subtracted the appropriate value of J from $\Delta\nu_{1/2}$. The major effect is with the ortho-couplings where J is ca. 8 Hz. We expect that the naphthalene ring protons $H_{19,}$ $H_{20,}$ $H_{21,}$ and H_{23} will have the same value of $\Delta\nu_{1/2}$because

Table 4. The effect of NaCl concentration on K and δ_{agg} fitted using the isodesmic model over all data points.

	H_{20}		H_{23}		$H_{24,26}$	
	δ_{mon}/ppm 8.625		δ_{mon}/ppm 6.820		δ_{mon}/ppm 7.867	
NaCl M	K/m^{-1}	δ_{agg}/ppm	K/m^{-1}	δ_{agg}/ppm	K/m^{-1}	δ_{agg}/ppm
0[a]	34.1/312		36.6/301	5.144/5.352	36.1/311	
1×10^{-5}	95.1	6.789	115	5.366	117	6.145
1×10^{-4}	151	6.966	113	5.366	156	6.189
1×10^{-3}	152	6.962	120	5.366	117	6.138
1×10^{-2}	125	6.845	110	5.336	108	6.138
0.1	424	7.032	410	5.422	440	6.209
0.3	1030	7.050	722	5.406	781	6.174
1	1590	7.050	1120	5.407	1692	6.174
3	1658	6.939	12594	5.5870	15772	6.186

Note: [a]Fitted at both monomer and aggregate concentrations.

there is one major dipole–dipole coupling to provide the line broadening. In particular, H_{23} is well-separated from the other resonances, and has been employed for $\Delta\nu_{1/2}$ measurements. However, because of the uncertainties introduced by the coalescence of broadened peaks, some of the estimated τ_c^S values will have errors of up to ca. 30%.

This relationship for T_2 has been used previously for surfactants to determine the size of the micelle provided the diffusion coefficient is known. However, it has been shown that τ_c^S alone can be used to distinguish between large ($\tau_c^S \sim 10^{-6}$ s) and smaller ($\tau_c^S \sim 10^{-9}$ s) micellar aggregates [26]. It must be noted that for Edicol, diffusion of the molecule along the stack is not possible and thus τ_c^S must be due to rotational diffusion, D_{r0}. The linewidths of the peaks increase from ca. 0.3 Hz at low concentration to 15 Hz at the highest concentration examined (T_2 = 1.6–0.01 s), equivalent to a hundred fold increase in τ_c^S ($10^{-10} \rightarrow 10^{-8}$ s) (Figure 7). The increase in $\Delta\nu_{1/2}$ becomes more marked above 10 wt% Edicol (ca. 2 Hz), reaching ca. 15 Hz at 23 wt%. Thus, a crude estimation of size can be made if we assume rod-like aggregates and that $1/\tau_c^S \approx D_{r0} \approx k_B T / 3\pi\eta_s \ln(L/d)/L^4$ [27] where η_s is the viscosity, L the length and d the diameter of the aggregate. This suggests that the largest aggregate size lies between 10 and 100 Å. There is good agreement between these estimates and previously reported sizes [12, 13, 15].

On addition of sodium chloride, a significant increase in line broadening occurs only at high NaCl concentrations, typically above 0.1 M (Figure 8). At 0.3 M the peaks of the 10 wt% solution are broadened to

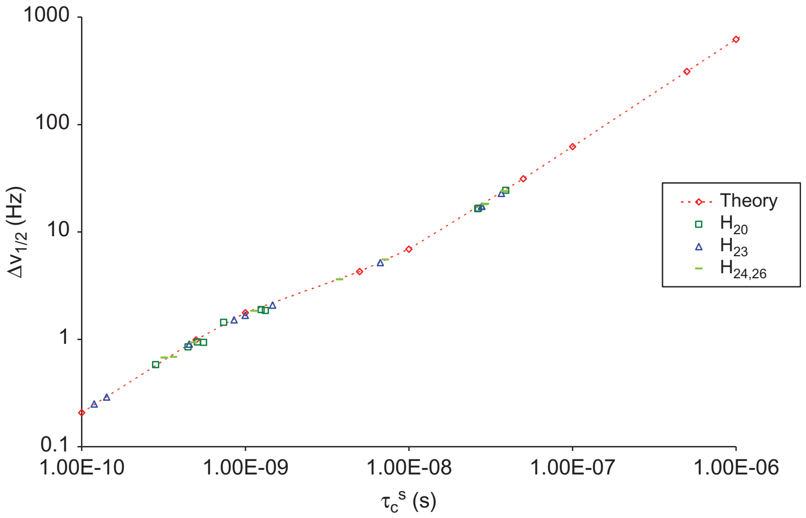

Figure 7. Pure Edicol: linewidth, $\Delta\nu_{1/2}$, as a function of the correlation time, τ_c^S, calculated from Equation (1) as indicated in the text (assuming $S = 0.6$ and an NMR frequency of 400 MHz) (colour version online).

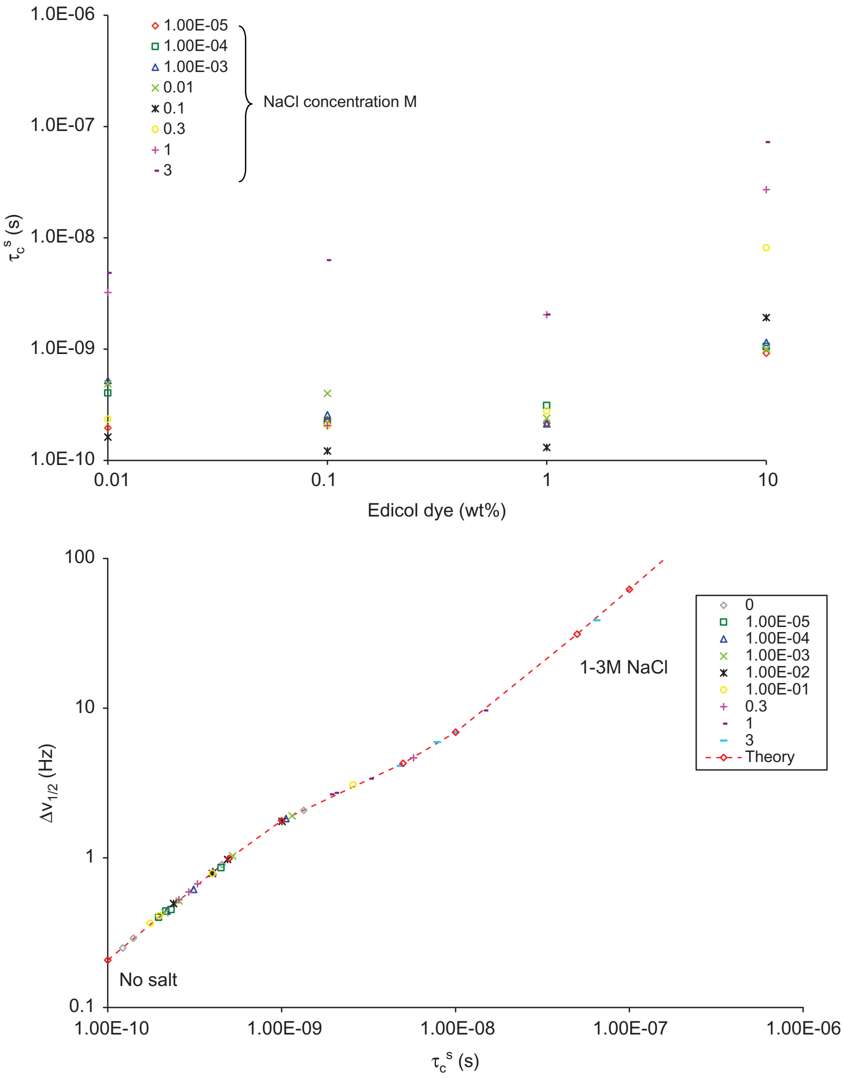

Figure 8. The effect of NaCl on the correlation time τ_c^S of Edicol (H_{23}) (colour version online).

ca. 5 Hz. However, at 1.0 M and 3.0 M even the 0.01 wt% solution has a $\Delta\nu_{1/2}$ of 4–5 Hz. Thus fairly large aggregates (ca. 3 nm) are present even in dilute solution where approximately half of the Edicol exists as free monomers. Clearly, the added electrolyte promotes the formation of larger stacks – probably due to the reduction of electrostatic repulsions.

4. Discussion and conclusions

The effects of added sodium chloride on mesophase stability are modest when compared to those that are observed in surfactant systems. Moderate levels (0.5 m) increase transition temperatures, while high levels reduce the temperatures. From the calculated monomer concentration based on chemical shifts, it seems likely that some of the stabilisation can be attributed to a small increase in stack volume fraction because of a reduced monomer concentration. The phase diagram of Edicol in water [2] shows that at ca. 35 wt% an increase in Edicol concentration of 1 wt% increases the mesophase transitions by 5°C. Furthermore, the density of sodium chloride solution is higher than that of water by 2 wt% for 0.5 M, increasing to 10 wt% for 3.0 M. Thus, the volume fraction of the solvent is smaller, so this will also act to increase the transition temperatures. These effects appear to be sufficient to account for the increase in mesophase stability at moderate electrolyte levels. The *decrease* in mesophase stability at the highest sodium chloride concentrations is very unexpected, and cannot be accounted for by this mechanism.

For the isotropic solutions, the absence of large changes in chemical shifts for sodium chloride concentrations less than 0.1 M shows that there are no dramatic changes in aggregation at 1 wt% Edicol or less. Hence long-range electrostatic repulsions (for example, between aggregates) do not influence the aggregation process. For these systems the Debye length is the same or larger than the stack size. Note that in 10 wt% Edicol the sodium ion concentration is ca. 0.2 M, which is equivalent to 0.1 M of a 1:1 electrolyte. However, the small see-saw effect in some of the chemical shifts suggests that the nature of the aggregates first formed changes with electrolyte concentration, as observed for the absence of electrolytes. This certainly is not to be expected from the isodesmic model.

There is no evidence for Edicol or other similar chromonic dye molecules possessing a nucleation or critical aggregation concentration similar to surfactant systems. However, it can be argued that the aggregation of the Edicol molecule does involve steric hindrance and electrostatic repulsion (a direct result of the two sulphate groups) with the head-to-tail dimer being the repeat unit in higher aggregate stacks [2]. It seems highly likely that intra-stack electrostatic repulsions play a part in preventing the aggregates from growing very large. The destabilisation of the mesophases at the highest Edicol and electrolyte concentrations is very surprising. We note that this cannot be attributed to any change in inter-molecular attractive forces due to any hydrophobic-type interactions because oil/water interfacial tensions are increased by the addition of inorganic salt, and hence mesophase stability would be increased. The origins of this behaviour must lie with changes in the electronic charge distribution around the aromatic rings, because the solvent has some different dielectric properties from water. We propose to investigate this possibility by the examination of Edicol mesophases in the presence of organic electrolytes and polar solutes such as urea.

Acknowledgements

We thank EPSRC and (the late) ICI for financial support. In addition, we are grateful to Professor A. Masters, Professor O. Lavrentovich, Dr L. Tortora, Dr O. Lozman, Dr C. Rodríguez-Abreu1, Dr M. Sintyureva and D.G. Edwards for valuable discussions. We also thank Professor M. Wilson and Dr F. Chami who provided details of unpublished structures from molecular simulations.

References

[1] Attwood, T.K.; Lydon, J.E.; Hall, C.; Tiddy, G.J.T. *Liq. Cryst.* **1990**, *7*, 657–668.

[2] Edwards, D.J.; Jones, J.W.; Lozman, O.; Ormerod, A.P.; Sintyureva, M.; Tiddy, G.J.T. *J. Phys. Chem. B* **2008**, *112*, 14628–14636.

[3] Ormerod, A.P. In *Chemistry*: Salford University: Salford, 1995.

[4] Collings, P.J.; Dickinson, A.J. *Liq. Cryst.* **2010**, *37*, 701–710.

[5] Yu, L.J.; Saupe, A. *Mol. Cryst. Liq. Cryst.* **1982**, *80*, 129–134.

[6] Yu, L.J.; Saupe, A. *Phys. Rev. Lett.* **1980**, *45*, 1000–1003.

[7] Martin, R.B. *Chem. Rev.* **1996**, *96*, 3043–3064.

[8] Chen, Z.J.; Lohr, A.; Saha - Moller, C.R.; Wurthner, F. *Chem. Soc. Rev.* **2009**, *38*, 564–584.

[9] Asakura, T.; Ishida, M. *J. Colloid Interface Sci.* **1989**, *130*, 184–189.

[10] Neumann, B.; Huber, K.; Pollmann, P. *Phys. Chem. Chem. Phys.* **2000**, *2*, 3687–3695.

[11] Neumann, B. *Langmuir* **2001**, *17*, 2675–2682.

[12] Tomasik, M.R.; Collings, P.J. *J. Phys. Chem. B* **2008**, *112*, 9883–9889.

[13] Horowitz, V.R.; Janowitz, L.A.; Modic, A.L.; Heiney, P.A.; Collings, P.J. *Phys. Rev. E: Stat., Nonlinear, Soft Matter Phys.* **2005**, *72*, 041710.

[14] Hamada, K.; Take, S.; Iijima, T.; Amiya, S. *J. Chem. Soc. – Faraday Trans. I* **1986**, *82*, 3141–3148.

[15] Park, H.S.; Kang, S.W.; Tortora, L.; Nastishin, Y.; Finotello, D.; Kumar, S.; Lavrentovich, O.D. *J. Phys. Chem. B* **2008**, *112*, 16307–16319.

[16] Budavari, S., O'Neill, M.J., Smith, A., Heckelman, P.E., Eds.; *Encyclopedia of Chemicals, Drugs, and Biologicals*, 11th ed. Merck Co, 1989.

[17] Kostko, A.F.; Cipriano, B.H.; Pinchuk, O.A.; Anisimov, M.A.; Danino, D.; Raghavan, S.R. *Abstr. Papers Am. Chem. Soc.* **2005**, *230*, U3030–U3031.

[18] Kostko, A.F.; Cipriano, B.H.; Pinchuk, O.A.; Ziserman, L.; Anisimov, M.A.; Danino, D.; Raghavan, S.R. *J. Phys. Chem. B* **2005**, *109*, 19126–19133.

[19] Skowronek, M.; Stopa, B.; Konieczny, L.; Rybarska, J.; Piekarska, B.; Szneler, E.; Bakalovski, G.; Roterman, I. *Biopolymers* **1998**, *46*, 267–281.

[20] Hamada, K.; Kubota, H.; Ichimura, A.; Iijima, T.; Amiya, S. *Ber. Bunsen-Ges.* **1985**, *89*, 859–863.

[21] Bracko, S.; Span, J. *Dyes Pigm.* **1997**, *35*, 165–169.

[22] Joshi, L.; Kang, S.W.; Agra-Kooijman, D.M.; Kumar, S. *Phys. Rev. E: Stat., Nonlinear, Soft Matter Phys.* **2009**, *80*, 041703-1-8.

[23] Wennerstrom, H.; Lindman, B.; Lindblom, G.; Tiddy, G.J.T. *J. Chem. Soc. – Faraday Trans. I* **1979**, *75*, 663–668.

[24] Lindblom, G.; Lindman, B.; Tiddy, G.J.T. *J. Am. Chem. Soc.* **1978**, *100*, 2299–2303.

[25] Manning, G.S. *Ann. Rev. Phys. Chem.* **1972**, *23*, 117–140.

[26] Staples, E.J.; Tiddy, G.J.T. *J. Chem. Soc. – Faraday Trans. I* **1978**, *74*, 2530–2541.

[27] Doi, M.; Edwards, S.F. *J. Chem. Soc. – Faraday Trans. II* **1978**, *74*, 560–570.